KnE Life Sciences
ICMScE
International Conference On Mathematics And Science Education
Volume 2024

Research Article

Electrical Properties of Gd- and Mn-Doped Fe_2O_3-$LaFeO_3$- La_2O_3 Thick Films for Ethanol Gas Sensors

Gizella Mentari Putri[1], Endi Suhend[1*], Muhamad Taufik Ulhakim[2], Andhy Setiawan[1], and Dani Gustaman Syarif[3]

[1]Physics Study Program, Universitas Pendidikan Indonesia, Jl. Dr. Setiabudi No. 229 Bandung, Indonesia
[2]Department of Mechanical Engineering, Faculty of Engineering, Universitas Buana Perjuangan Karawang, Jl. HS. Ronggo Waluyo, Karawang, Indonesia
[3]Center of Science and Technology of Applied Nuclear, National Nuclear Energy Agency of Indonesia (BATAN), Jl. Tamansari No. 71 Bandung, Indonesia

ORCID
Gizella Mentari Putri: https://orcid.org/0009-0006-0755-8914
Endi Suhendi: https://orcid.org/0000-0001-8256-8537
Muhamad Taufik Ulhakim: https://orcid.org/0000-0002-8812-8644
Andhy Setiawan: https://orcid.org/0000-0002-0922-3644

Corresponding Author: Endi Suhend; email: endis@upi.edu

Published: 27 March 2024

Publishing services provided by Knowledge E

Selection and Peer-review under the responsibility of the ICMScE Conference Committee.

Abstract.
Herein, electrical properties of ethanol gas sensing based on Gd- and Mn- doped Fe_2O_3-$LaFeO_3$-La_2O_3 thick films were investigated. The Gd- and Mn-doped Fe_2O_3-$LaFeO_3$-La_2O_3 were synthesized by coprecipitation method and formed to thick films using screen-printing techniques with sintering temperature at 900 °C. X-ray diffraction and scanning electron microscopy were conducted to determine the crystal and morphological structures. The results showed that the synthesized materials have three phases i.e., tetragonal, cubic, and hexagonal, respectively for Fe_2O_3-$LaFeO_3$-La_2O_3. Also, the average particle size is of about 0.51 μm. Among all those circumstances, synthesized materials indicate good performances as ethanol gas sensing that showed in the electrical properties' measurement. It tested A differently in ethanol containing i.e., 0 ppm, 100 ppm, 200 ppm, and 300 ppm. The highest response to ethanol gases reached at 300 ppm, it is 332 with optimum temperature at 289 °C. We hope our findings could be beneficial and helpful in the perfect fabrication of ethanol gas sensors in future.

Keywords: electrical properties, thick films, doped, ethanol, sensors

1. INTRODUCTION

Nowadays, the pollution in the form of liquids, solids, or gasses which are produced from the industrial field have become an alarming situation around the world. The several pollutants are toxic gasses such as nitrogen dioxide, acetone, methanol, ammonia, and ethanol. From all of them, ethanol is the important concern because it is considered to have an adverse effect on human beings and has a long-term exposure that leads to several diseases including cardiovascular and respiratory infection [1]. It is due to the ethanol characteristic that is easy to volatilize into air [2]. To solve the problem, the researchers has been developed gas sensors to detect the ethanol in the air and minimize the negative impact that might occurred. Some of the researchers established the ethanol gas sensor using metal oxide semiconductor (MOS) due to their higher response. MOS that are widely used as ethanol gas sensors are ZnO, Co_3O_4, SnO_2, MoO_3, $LaFeO_3$, and so on [3–7]. It becomes interesting to choose a good type of MOS for ethanol gas sensor applications.

Recently, LaFeO3 has attracted much attention to applied as ethanol gas sensors due to their electrical properties. $LaFeO_3$ belongs to ABO_3perovskite-structured oxide materials that have many advantages, especially has an excellent response and stability [8]. Therefore, some of method has been developed to produced $LaFeO_3$ in-between sol-gel, solvothermal, and coprecipitation [9–11]. However, the researchers were convinced that coprecipitation is the most suitable method to produce LaFeO3 for ethanol gas sensors due to their superiority. The coprecipitation method can produce materials in a small grain sizes or nanoparticle [12]. For gas sensors applications, a small grain sizes exhibited the higher response and giving a good performance to detect the targets [13]. Also, Suhendi et al claimed that to produce a small grain size can be obtained with added doping. Their work proven that SrO doping on $LaFeO_3$ decreased the grain sizes of about 0.42 μm to 0.26 μm [14]. The other researchers also applied doping for gas sensors application. An example, Gd-doping ZnO that was conducted by Colak and Karakose (2022). Their work claimed that 3 mol% of Gd-doping ZnO increased the performance in detecting the target gasses [15]. Furthermore, Suhendi et al (2020) also added 0.17 wt% Mn-doping to $LaFeO_3$ and found that the response of gas sensors was increased of about 6.98 to 23.89 in 300 ppm ethanol gasses containing [16]. Based on the previously report, this work was attempt to combine the doping i.e. Gd and Mn to $LaFeO_3$. It was conducted with the aim to produce a good performance of ethanol gas sensors.

Here in, the Gd and Mn doping to $LaFeO_3$ was made into thick film ceramics using screen-printing techniques caused by several reasons such as low-cost, easy in preparation, and can improve the surface area which can be a benefit for gas sensing application[17]. Also, in this work we used the La_2O_3 precursor and $Fe_2O_3$from the yarosite minerals extraction to utilize the natural resources of Indonesia, so that the final material that we used to detect the ethanol gasses is Gd-and Mn-doped Fe_2O_3-$LaFeO_3$-La_2O_3 thick film ceramics. Then, some characterization including crystal structure, morphological structure, and electrical properties were conducted to verify their performance. Hoping all the findings of this work can be a useful thing for the development of ethanol gas sensors.

2. RESEARCH METHOD

This research was conducted by several steps including the synthesized of Gd-and Mn-doped Fe_2O_3-$LaFeO_3$-La_2O_3 powders, screen-printing techniques to form these powders into thick films, and characterization to reveal their performance as ethanol gas sensors. The synthesized of Gd-and Mn-doped Fe_2O_3-$LaFeO_3$-La_2O_3 powders was prepared by coprecipitation method in accordance with the experiment that has been done by Suhendi et al in 2021 [18]. Firstly, the precursor that consist of 46 mol% Lanthanum Oxide (La2O3), 46 mol% Ferric Oxide (Fe2O3) from yarosite extraction, 5 mol% Manganese Oxide (Mn2O3), and 3 mol% Gadolinium Oxide (Gd2O3) were prepared. All the precursors respectively dissolved in Hydrochloric Acid (HCl) 10 M using a magnetic stirrer for about 5 hours. Each solution that was produced was mixed until it became a homogeneous solution. Then, the Ammonia Hydroxide (NH4OH) was added until the solution produced the precipitate. The precipitate dried at 100 °C for about 6 hours and calcined at 600 °C for about 3 hours. Lastly, the products were grinded to become powders.

The powders that were produced were formed into thick films using screen printing techniques as illustrated in Figure 1. This approach required several materials such as alumina substrate, silver (Ag) paste, and organic vehicles that consist of ethyl cellulose and alpha-terpineol in the ratio 1:9. Firstly, the material paste was prepared by mixing the Gd-and Mn-doped Fe_2O_3-$LaFeO_3$-La_2O_3 powder and organic vehicle in the composition ratio of 7:3. These mixtures are stirred for about 2 hour or until homogeneous. Then, alumina substrate is also prepared in the size of 1 cm x 0.5 cm as illustrated in Figure 1a. After that, the silver (Ag) paste was coated over the alumina substrate and fired at 600 °C for about 10 minutes as illustrated in Figure 1b. The silver (Ag) paste is used as an electrode in the ethanol gas detection processes. The last step is to print the material paste over the alumina substrate that has been coated with silver (Ag) paste previously as illustrated in Figure 1c and fired at 900 °C for about 2 hours.

Hereafter, the thick films based on Gd-and Mn-doped Fe2O3-LaFeO3-La2O3 were characterized using x-ray diffraction (XRD) and scanning electron microscopy (SEM) to determine their crystal and morphological structures. The XRD characterization were conducted using PANanalytical X'Pert PRO seri PW3040/X0 and informed the crystal structure that obtained from the XRD graphical pattern that formed from the intensity and the angle of bragg diffraction which matched to the literatures. Then, the crystallite size is also informed which is obtained from the calculation using Debye-Scherrer equation as shown in Equation 1 [19–22].

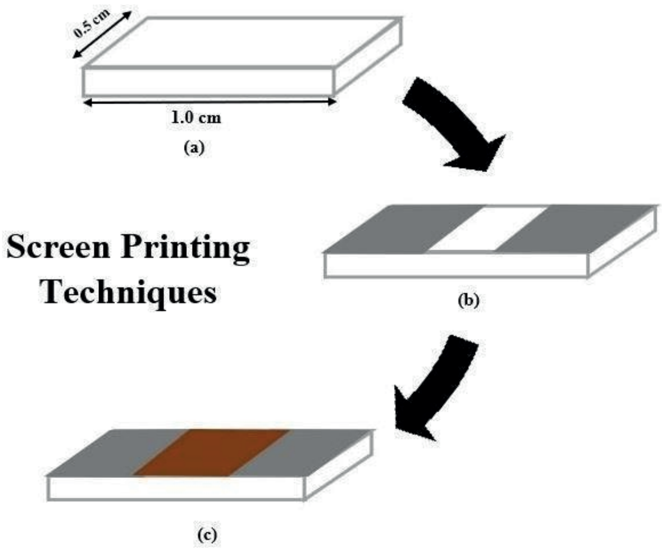

Figure 1: The process of screen printing techniques, including (a) The size of alumina substrate (b) Silver (Ag) coating (c) Material paste coating.

To use this “Old Style Equation” as a “template,” highlight the entire line, then use cut and paste to the new location. Note that the equation number will automatically update (increment).

$$D = \frac{0.89\lambda}{B\ coscos\ \theta}(1)$$

Where λ is a wavelength of the x-ray sources (this characterization was use Cu $K\alpha$ = 1.5404 x 10-10 m), B is the intensity of peak of full width at half-maximum (FWHM), and θ is the angle of Bragg diffraction that use in the characterization. Meanwhile, SEM characterization was conducted using JEOL JSM 6360 LA and informed the image with a certain magnification. This characterization confirmed the particle size of Gd-and Mn-doped Fe_2O_3-$LaFeO_3$-La_2O_3. Then, the third characterization is electrical properties investigation that is conducted to ensure the Gd-and Mn-doped Fe_2O_3-$LaFeO_3$-La_2O_3 based thick film performances on the detection of ethanol gases. The electrical properties were characterized using a static gas chamber in three variations of ethanol gas concentration i.e. 0 ppm, 100 ppm, 200 ppm, and 300 ppm. This characterization informed the performance of gas sensors including response and operating temperature. The response was known from the resistance value at various temperatures shown in the R-T graphic which is processed with the calculation using Equation 2 [23–27].

$Respon = \frac{R_g}{R_a}$ x 100% (2)

where Rg is the resistance value of gas sensors in the ethanol gas containing and Ra is the resistance value at ambient condition (without ethanol gas).

3. RESULTS AND DISCUSSION

In this work, we conducted the characterization of Gd-and Mn-doped Fe_2O_3-$LaFeO_3$-La_2O_3 thick film ceramics as the proponent data for their electrical properties as ethanol gas sensors. These characterizations respectively are XRD and SEM. XRD were used to determine the crystal characteristics including crystal structure, lattice parameter, and crystallite size of Gd-and Mn-doped Fe_2O_3-$LaFeO_3$-La_2O_3. These characteristics were known with the analysis that conducted to the XRD pattern shown in Figure 2. The analysis were carried out using Match3! and confirmed that the materials has three phase i.e. Fe_2O_3, $LaFeO_3$, and La_2O_3. It is respectively fitted with the Inorganic Crystal Structure Database (ICSD) No. 00-033-0664, 98-003-2636, and 96-006-9890. Each phase has a different crystal structure, there are tetragonal for Fe_2O_3, cubic for $LaFeO_3$, and hexagonal for La_2O_3.

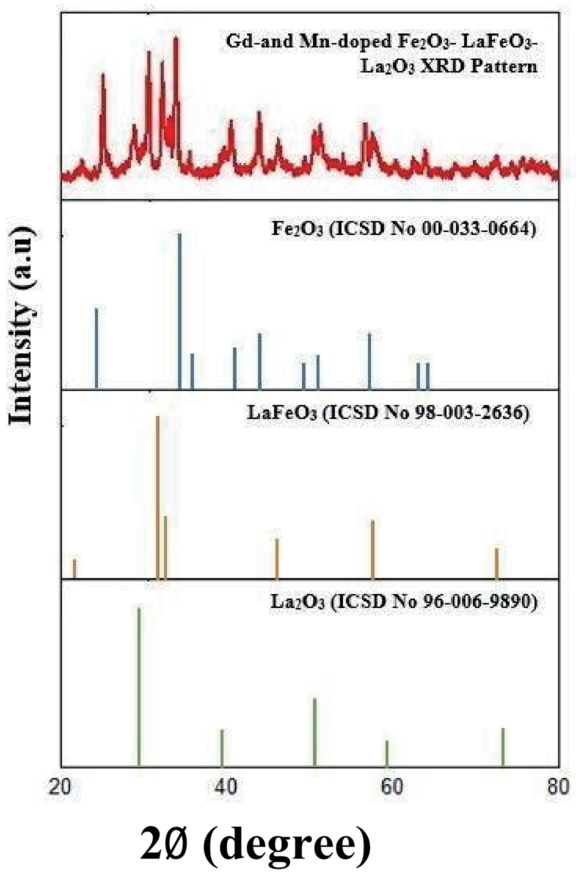

Figure 2: XRD pattern of Gd-and Mn-doped Fe_2O_3-$LaFeO_3$-La_2O_3.

The analysis also informed the lattice parameter and crystallite size for each phase that respectively shown in Table 1. The lattice parameters were known from the analysis using match 3!, meanwhile the crystallite size was known from the calculation using Debye-Scherrer formula that shown in Equation 1. The crystallite size has an influence on the materials performance as gas sensors. A small crystallite size provides a better response of the sensors to detect the targets, including on the detecting or recognizing the ethanol as the targets [28].

Table 1: The lattice parameters and crystallite size for each phase of Gd-and Mn-doped Fe_2O_3-$LaFeO_3$-La_2O_3.

Phase	Lattice Parameters (Å)			Crystallite Size (nm)
	a	b	c	
Fe_2O_3	8.481	8.481	25.677	21.8
$LaFeO_3$	3.926	3.926	3.926	10.2
La_2O_3	3.631	3.631	5.865	14.2

Then, from the XRD pattern also formed the other peaks outside of the ICSD fitted. These peaks might be formed from the impurities that brought from the Fe_2O_3 precursor. In this work, the Fe_2O_3 precursor that used were from the yarosite mineral extraction. These impurities were consist of several compound that shown in Table 2 as reported by Ariyani et al at 2017 [29].

Table 2: The impurities on the Fe_2O_3 precursor from yarosite mineral extraction.

No.	Compound	wt%
1	Fe_2O_3	91.30
2	Al_2O_3	3.30
3	SiO_2	2.05
4	TiO_2	3.02
5	CaO	0.16
6	MnO	0.17

Hereinafter, the SEM characterization was conducted to determine the average particle size of Gd-and Mn-doped Fe2O3-LaFeO3-La2O3. The result of SEM characterization is an image with a certain magnification as shown in Figure 3. From the analysis, it is known that the average particle size of Gd-and Mn-doped Fe2O3-LaFeO3-La2O3 is about 0.51 μm. These sizes make an impact on their performance as ethanol gas sensors, it seems like the results obtained from the electrical properties measurements.

The electrical properties measurements were conducted to ensure the performance of Gd-and Mn-doped Fe2O3- LaFeO3-La2O3 on detecting the ethanol gas as target. The electrical properties were conducted with resistance measurement using an

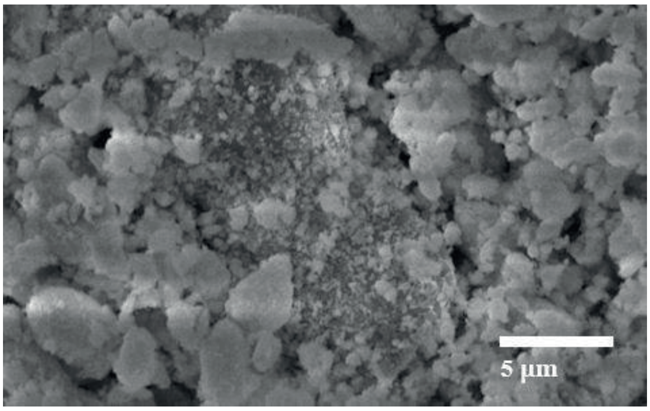

Figure 3: SEM characterization image of Gd-and Mn-doped Fe_2O_3-$LaFeO_3$-La_2O_3.

ohmmeter in every 3 °C increment of temperature until obtained the R-T graphic as shown in Figure 4a. The measurements informed that the resistance decreased as the temperature increased. Also, the resistance at the same temperature increased as the ethanol gas concentration increased. It occurred when the thick film surfaces were exposed to the ethanol gasses, the absorbed oxygen reacted with the ethanol by releasing the trapped electrons to the Gd-and Mn-doped Fe2O3-LaFeO3-La2O3. These interaction were explained in the Equation 3 [30].The ethanol concentrations that were used in the measurement are 0 ppm, 100 ppm, 200 ppm, and 300 ppm.

C2H5OH (gas) + 6O$^-$ ↔ 2CO2 + 3H2O + 6e$^-$ (3)Then, Srinivasan et al (2019) revealed if the resistance of the materials semiconductor were higher in the ethanol gas contain than in the without ethanol gas (ambient condition), the materials accordingly to the p-type semiconductor [31]. It confirmed that the Gd-and Mn-doped Fe_2O_3-$LaFeO_3$-La_2O_3 that produced in this work are p-type semiconductors.

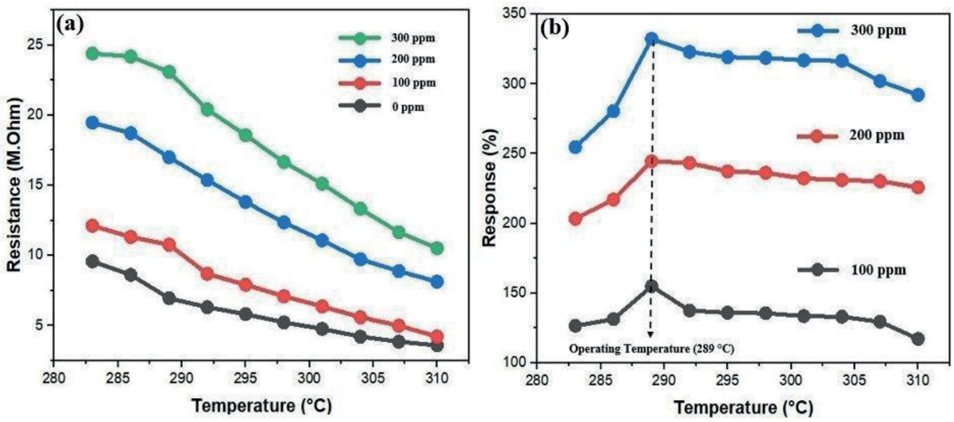

Figure 4: (a) The resistance and (b) The response of Gd-and Mn-doped Fe2O3-LaFeO3-La2O3.

The resistance that produced the measurement was calculated using Equation 2. These calculations informed the response value of Gd-and Mn-doped Fe_2O_3-$LaFeO_3$-La_2O_3 on detecting the ethanol gas as shown in Figure 4b. An optimum response was reached in the 300 ppm, it is about 332 with the optimum temperature of about 289 °C. The value of response is included to a good performance of Gd-and Mn-doped Fe_2O_3-$LaFeO_3$-La_2O_3. It is possible from doping that it provides a strong effect. Hu et al (2017) claimed that a good performance was obtained from a different characteristic of the doping, also the doping can help the main materials to bind the oxygen atoms that contain in the ethanol gasses. These processes can increase the responses [32].

These processes are also explained by the sensing mechanism of Gd-and Mn-doped Fe_2O_3-$LaFeO_3$-La_2O_3 on detecting the ethanol gasses. The sensing mechanisms were adsorption and desorption of gas molecules on the thick film surface. It shown by the reaction in Equation 4 to 6 [33].

O2 (gas) ↔ O2 (ads) (4)

O2 (ads) + e^- (CB) ↔ O $^-$ (ads) (5)

O $^-$ (ads) + e^- (CB) ↔ 2O^- (ads) (6)

4. CONCLUSION

An electrical properties of Gd-and Mn-doped Fe2O3-LaFeO3-La2O3 thick films has been successfully investigated. In the first, we have to prepare the powders of Gd-and Mn-doped Fe_2O_3-$LaFeO_3$-La_2O_3 by coprecipitation method and formed to thick films using screen-printing techniques. Then, the characterizations were conducted using XRD and SEM to espouse the materials performance as ethanol gas sensors. These characterization were obtained the three phase of crystal structure i.e. tetragonal, cubic, and hexagonal. Also, infomed the average of particle size of about 0.51 µm. Lastly, the analysis of the electrical properties of Gd-and Mn-doped Fe_2O_3-$LaFeO_3$-La_2O_3 -based thick films revealed a good performance as ethanol gas sensors with the highest response 332 (300 ppm) and operating temperature at 289 °C.

Acknowledgments

This work was financially supported by “Hibah Penelitian Terapan Unggulan Perguruan Tinggi” Kementerian Riset, Teknologi dan Pendidikan Tinggi Republik Indonesia Research Grants in the fiscal year 2021.

References

[1] Umar A, Ibrahim AA, Nakate UT, Albargi H, Alsaiari MA, Ahmed F, et al. Fabrication and characterization of CuO nanoplates based sensor device for ethanol gas sensing application. Chem Phys Lett. 2021;763:138204.

[2] Zhang K, Qin S, Tang P, Feng Y, Li D. Ultra-sensitive ethanol gas sensors based on nanosheet-assembled hierarchical ZnO-In_2O_3 heterostructures. J Hazard Mater. 2020 Jun;391:122191.

[3] Wang C, Wang ZG, Xi R, Zhang L, Zhang SH, Wang LJ, et al. In situ synthesis of flower-like ZnO on GaN using electrodeposition and its application as ethanol gas sensor at room temperature. Sens Actuators B Chem. 2019;292:270–6.

[4] Gong Y, Wang Y, Sun G, Jia T, Jia L, Zhang F, et al. Carbon nitride decorated ball-flower like Co_3O_4 hybrid composite: hydrothermal synthesis and ethanol gas sensing application. Nanomaterials (Basel). 2018 Feb;8(3):132.

[5] Elger AK, Hess C. Elucidating the mechanism of working SnO2 gas sensors using combined operando UV/Vis, Raman, and IR spectroscopy. Angew Chem Int Ed Engl. 2019 Oct;58(42):15057–61.

[6] Zhu L, Zeng W, Li Y, Yang J. Enhanced ethanol gas-sensing property based on hollow MoO_3 microcages. Physica E. 2019;106:170–5.

[7] Hao P, Qiu G, Song P, Yang Z, Wang Q. Construction of porous $LaFeO_3$ microspheres decorated with NiO nanosheets for high response ethanol gas sensors. Appl Surf Sci. 2020;515:146025.

[8] Xiang J, Chen X, Zhang X, Gong L, Zhang Y, Zhang K. Preparation and characterization of Ba-doped LaFeO3 nanofibers by electrospinning and their ethanol sensing properties. Mater Chem Phys. 2018;213:122–9.

[9] Theingi M, Tun KT, Aung NN. Preparation, characterization and optical property of $LaFeO_3$ nanoparticles via sol-gel combustion method. SciMedicine Journal. 2019;1(3):151–7.

[10] Zhang T, Guo Y, Li C, Li Y, Li J, Zhao F, et al. The effect of $LaFeO_3$@ MnO_2 on the thermal behavior of energetic compounds: an efficient catalyst with core-shell structure. Adv Powder Technol. 2020;31(11):4510–6.

[11] Salah LM, Haroun M, Rashad MM. Structural, magnetic, and electrical properties of Gd-substituted LaFeO 3 prepared by co-precipitation method. Journal of the Australian Ceramic Society. 2018;54(2):357–68.

[12] Peng Y, Xia C, Cui M, Yao Z, Yi X. Effect of reaction condition on microstructure and properties of (NiCuZn)Fe_2O_4 nanoparticles synthesized via co-precipitation with ultrasonic irradiation. Ultrason Sonochem. 2021 Mar;71:105369.

[13] Zhang D, Yang Z, Yu S, Mi Q, Pan Q. Diversiform metal oxide-based hybrid nanostructures for gas sensing with versatile prospects. Coord Chem Rev. 2020;413:213272.

[14] Suhendi E, Ulhakim MT, Setiawan A, Syarif DG. The effect of SrO doping on LaFeO3 using yarosite extraction based ethanol gas sensors performance fabricated by coprecipitation method. International Journal of Nanoelectronics and Materials. 2019;12(2):185–92.

[15] Çolak H, Karaköse E. Gadolinium (III)-doped ZnO nanorods and gas sensing properties. Mater Sci Semicond Process. 2022;139:106329.

[16] E. Suhendi, M.T.U. Latifah, A. Setiawan, and D.G. Syarif, "Studies on the effect of MnO doping on $LaFeO_3$ Ceramics in Comparison to Yarosite Mineral Properties for Ethanol Gas Sensors Performance.," *International Journal of Nanoelectronics & Materials*. vol. 14, no. 4, p. 2021.

[17] Powar RR, Parale VG, Phadtare VD, Wategaonkar SB, Mane RK, Gunjkar JL, et al. Nanocrystalline spinel zinc-substituted cobalt ferrite thick film an efficient ethanol sensor. Mater Today Chem. 2021;22:100607.

[18] Suhendi E, Amanda ZL, Ulhakim MT, Setiawan A, And DG. Syarif, "The enhancement of ethanol gas sensors response based on calcium and zinc co-doped LaFeO3/Fe2O3 thick film ceramics utilizing yarosite minerals extraction as Fe2O3 precursor.," *Journal of Metals*. Materials and Minerals. 2021;31(2):71–7.

[19] Saadat Niavol S, Milani Moghaddam H. SnO 2 nanoparticles/reduced graphene oxide nanocomposite for fast ethanol vapor sensing at a low operating temperature with an excellent long-term stability. J Mater Sci Mater Electron. 2021;32(5):6550–69.

[20] Raji P, Kumar KB. Investigation of Ti doping on the structural, optical, and magnetic properties of ZnO nanoparticles. J Mater Sci Mater Electron. 2021;32(9):11751–62.

[21] Ghobadifard M, Farhadi S, Mohebbi S. Catalytic performance of ZnFe 2 O 4 nanoparticles prepared from the [ZnFe 2 O (CH 3 COO) 6 (H 2 O) 3]· 2H 2 O complex under microwave irradiation. Res Chem Intermed. 2019;45(2):379–400.

[22] Yadav N, Singh A, Kaushik M. Hydrothermal synthesis and characterization of magnetic Fe_3O_4 and APTS coated Fe_3O_4 nanoparticles: physicochemical investigations of interaction with DNA. J Mater Sci Mater Med. 2020 Jul;31(8):68.

[23] Suhendi E, Putri AE, Ulhakim MT, Setiawan A, Syarif DG. “Investigation of ZnO doping on $LaFeO_3$ / Fe_2O_3 prepared from yarosite mineral extraction for ethanol gas sensor applications.,” *AIMS Materials Science*. vol. 9, no. 1, p. 2022.

[24] Wang Z, Li F, Wang H, Wang A, Wu S. An enhanced ultra-fast responding ethanol gas sensor based on Ag functionalized CuO nanoribbons at room-temperature. J Mater Sci Mater Electron. 2018;29(19):16654–9.

[25] Mahmood MH, Maleque MA. Effective parameter of Nano-CuO coating on CO gas-sensing performance and heat transfer efficiency. Arab J Sci Eng. 2021;46(7):6557–66.

[26] Mehmood S, Zhao X, Bhopal MF, et al. MoO_2-Ni-graphene ternary nanocomposite for a high-performance room-temperature ethanol gas sensor. Appl Surf Sci. 2021;554:149595.

[27] Li P, Cao C, Shen Q, Bai B, Jin H, Yu J, et al. Cr-doped NiO nanoparticles as selective and stable gas sensor for ppb-level detection of benzyl mercaptan. Sens Actuators B Chem. 2021;339:129886.

[28] Zhou Q, Chen W, Xu L, Kumar R, Gui Y, Zhao Z, et al. Highly sensitive carbon monoxide (CO) gas sensors based on Ni and Zn doped SnO2 nanomaterials. Ceram Int. 2018;44(4):4392–9.

[29] Ariyani NI, Syarif DG, Suhendi E. “Fabrication and Characterization of Thick Film Ceramics La0, 9Ca0, 1FeO3 for Ethanol Gas Sensor using Extraction of Fe_2O_3 from Yarosite Mineral.,” In: *IOP Conference Series: Materials Science and Engineering*. pp. 12037. *IOP Publishing* (2018).

[30] Liu C, Navale ST, Yang ZB, Galluzzi M, Patil VB, Cao PJ, et al. Ethanol gas sensing properties of hydrothermally grown α-MnO_2 nanorods. J Alloys Compd. 2017;727:362–9.

[31] Srinivasan P, Ezhilan M, Kulandaisamy AJ, Babu KJ, Rayappan JB. Room temperature chemiresistive gas sensors: challenges and strategies—a mini review. J Mater Sci Mater Electron. 2019;30(17):15825–47.

[32] Hu X, Zhu Z, Chen C, Wen T, Zhao X, Xie L. Highly sensitive H_2S gas sensors based on Pd-doped CuO nanoflowers with low operating temperature. Sens Actuators B Chem. 2017;253:809–17.

[33] A. Mirzaei, J.-H. Lee, S.M. Majhi, et al., “Resistive gas sensors based on metal-oxide nanowires.,” *Journal of Applied Physics*. vol. 126, no. 24, p. 2019. https://doi.org/10.1063/1.5118805.